The Brazilian Amaryllidaceae as a source of acetylcholinesterase inhibitory alkaloids

Jean Paulo de Andrade . Raquel B. Giordani . Laura Torras-Claveria .Natalia Bele´n Pigni . Strahil Berkov . Merce` Font-Bardia . Teresa Calvet . Eduardo Konrath . Kelly Bueno . Liana G. Sachett . Julie H. Dutilh . Warley de Souza Borges . Francesc Viladomat . Amelia T. Henriques . Jerald J. Nair . Jose´ Angelo S. Zuanazzi . Jaume Bastida

J. P. de Andrade · L. Torras-Claveria ·
N. B. Pigni · S. Berkov · F. Viladomat ·
J. J. Nair · J. Bastida
Departament de Productes Naturals, Biologia Vegetal i Edafologia, Facultat de Farma`cia, Universitat de Barcelona, Av. Diagonal 643, 08028 Barcelona, Spain
e-mail: jaumebastida@ub.edu

J. P. de Andrade · R. B. Giordani · E. Konrath ·
K. Bueno · L. G. Sachett A. T. Henriques ·
J. A. S. Zuanazzi
Faculdade de Farma´cia, Universidade Federal do Rio Grande do Sul, 2752 Ipiranga Av.,
Porto Alegre 90610-000, Brazil

J. P. de Andrade · W. de Souza Borges
Departamento de Quı´mica, Universidade do Espı´rito Santo, Vitoria, ES 29075-910, Brazil

S. Berkov
AgroBioInstitute, 8 Dragan Tzankov blvd., 1164 Sofia, Bulgaria

M. Font-Bardia
Centres Cientifics i Tecnologics, Universitat de Barcelona, Sole´ i Sabaris 1-3, 08028 Barcelona, Spain

T. Calvet
Cristal.lografia, Mineralogia i Dipo`sits Minerals, Facultat de Geologia, Universitat de Barcelona, Martı´ i Franque`s s/n, 08028 Barcelona, Spain

J. H. Dutilh
Departamento de Botaˆnica, Universidade de Campinas, Cidade Universita´ria, Campinas 13083-970, Brazil

ABSTRACT:

Nine Brazilian Amaryllidaceae species were studied for their alkaloid composition and acetylcholinesterase (AChE) inhibitory activity via GC–MS and a modified Ellman assay, respectively. A total of thirty-six alkaloids were identified in these plants, of which Hippeastrum papilio and H. glaucescens exhibited the highest galanthamine content and the best IC50 values against AChE. Furthermore, Hippeastrum vittatum and Rhodophiala bifida also showed notable AChE inhibitory effects. X-ray crystallographic data for four galanthamine-type compounds revealed significant differences in the orientation of the N-methyl group, which are shown to be related to AChE inhibition.

INTRODUCITON

The Amaryllidaceae alkaloids represent a large group of isoquinoline alkaloids derived from the common biogenetic precursor O-methylnorbelladine through oxidative phenolic coupling, leading to eight distinct structural-types (Bastida et al. 2006). The galanthamine- type skeleton has been the focus of numerous studies since the AChE inhibitor galanthamine was approved by the FDA for the clinical management of mild to moderate Alzheimer's disease (AD) (Maelicke et al. 2001). Although the chemical synthesis of galanthamine has been achieved on several occasions, natural sources still constitute the bulk of its commercial supply chain (Berkov et al. 2011). Apart from this, the other structural representatives of the Amaryllidaceae are known for a diverse array of biological activities including, antitumoral, antiviral, antiparasitic, anti-inflammatory, psychopharmacological and interactions with human cytochrome P450 3A4 (Vrijsen et al. 1986; C¸ itog˘lu et al. 1998; da Silva et al. 2006; McNulty et al. 2007, 2009; Zupko´ et al. 2009; Giordani et al. 2010). These attributes have showcased the Amaryllidaceae as a promising resource for new and bioactive molecules.

The high resolution power of the capillary column technique in gas chromatography (GC) together with the ready availability of libraries of electron impact mass spectrometry (EI–MS) data in the literature facilitate the rapid identification and quantification of known alkaloids. This has been shown to be particularly useful to studies of the Amaryllidaceae, extracts of which contain a large number of alkaloids (Kreh et al. 1995; Wagner et al. 2003). To this extent, several southern Brazilian Amaryllidaceae species have been examined for their alkaloid content and biological activity (da Silva et al. 2006, 2008; Pagliosa et al. 2010; Giordani et al. 2011a, b; de Andrade et al. 2011). In the present study, a GC–MS analysis was undertaken on nine Amaryllidaceae species which allowed for the identification of thirty-six alkaloids belonging to seven skeleton-types. Furthermore, an AChE inhibitory activity assay was carried out with both isolated compounds and alkaloid-rich fractions. In addition, X-ray crystallographic analysis was carried out on some galanthamine derivatives, providing insights to the structural features attending AChE activity.

MATERIALS AND METHODS

Chemicals

Galanthamine (27) and 11b-hydroxygalanthamine (32) used for X-ray crystallography were previously obtained from Hippeastrum papilio (de Andrade et al. 2011). Sanguinine (28) and narwedine (31) were obtained in previous works from Crinum kirkii Chemicals Galanthamine (27) and 11b-hydroxygalanthamine (32) used for X-ray crystallography were previously obtained from Hippeastrum papilio (de Andrade et al. 2011). Sanguinine (28) and narwedine (31) were obtained in previous works from Crinum kirkii (Machocho et al. 2004) and Leucojum aestivum (Berkov et al. 2008a), respectively. MeOH (HPLC grade), CHCl3, Me2CO, H2SO4 and NH4 ? (analytical grade) were purchased from SDS (France). Acetylthiocholine iodide (ATCI), acetylcholinesterase (AChE) from electric eels (type VI-S lyophilized powder), and 5,5 V-dithiobis[2-nitrobenzoic acid] (DTNB) were obtained from Sigma-Aldrich Chemie (Steinheim, Germany). The n-hydrocarbon mixture (C9–C36, Restek, Cat no. 31614) was supplied by Teknokroma (Spain). Galanthamine (purity[99 %) used for the calibration curves was previously obtained by the authors, and codeine (purity C 99 %) used as internal standard was purchased from Sigma Aldrich (St. Louis, MO, USA).

Plant material

The species H. papilio (Ravenna) Van Scheepen (bulbs and leaves, UFRGS–ICN 149428), Hippeastrum vitattum (L'He´r.) Herb. (bulbs, UFRGS–ICN 8889), Hippeastrum striatum (Lam.) Moore (bulbs, UFRGS–ICN 9549), Hippeastrum morelianum Lem. (bulbs, UNICAMP–UCE 14351), Hippeastrum santacarina (Traub) Dutilh (bulbs, UFRGS–ICN 149429), Hippeastrum breviflorum Herb. (bulbs, UFRGS–ICN 9190), Hippeastrum glaucescens (Mart.) Herbert (bulbs and leaves, UFRGS–ICN 8894), Hippeastrum psittacinum Herb. (bulbs and leaves, UNICAMP–UCE 143513) and Rhodophiala bifida (Herb.) Traub (bulbs, UNICAMP–UCE 136352) were collected and the extracts obtained according to previously described methods (Castilhos et al. 2007; da Silva 2005; da Silva et al. 2008; Pagliosa et al. 2010; Giordani et al. 2011a, b; de Andrade et al. 2011; Sebben 2005).

Sample preparation

The plant material (1 g) was crushed and extracted by stirring at rt with MeOH (3 9 50 ml), the combined macerate filtered and evaporated to dryness under reduced pressure. The crude extract was acidified to pH 2 with 2 % H2SO4, neutral material removed using Et2O (3 9 25 ml). The aqueous phase was then basified up to pH 11 with NH3 (25 %, v/v) and extracted with CHCl3 (3 9 25 ml) to afford the chloroform extract.

GC–MS and identification of alkaloids

The chloroform extract (300 ll) was filtered and then used for subsequent GC–MS analysis. EI–MS spectra were obtained on an Agilent 6890 N GC 5975 inert MSD operating in EI mode at 70 eV (Agilent Technologies, Santa Clara, California, USA) utilizing a DB-5 MS column (30 m 9 0.25 mm 9 0.25 lm, Agilent Technologies) with an injector temperature of 280 C. The temperature program was as follows: 100–180 C at 15 Cmin-1, 1 min hold at 180 C and 180–300 C at 5 Cmin-1 and 10 min hold at 300 C. The flow rate of carrier gas (Helium) was 0.8 ml min-1 and a split ratio of 1:20 was followed. The alkaloids were identified by comparing their GC–MS spectra and Kovats retention indices (RI) with our in-house library database. This library has been continually updated and reviewed with alkaloids isolated by our group and identified using other spectroscopic techniques such as NMR, UV, CD and MS. Mass spectra were deconvoluted using AMDIS 2.64 software (NIST). Kovats retention indexes (RI) of the compounds were recorded with standard calibration of an n-hydrocarbon mixture (C9–C36).

The proportion of each individual component in the alkaloid fractions analysed by GC–MS (Table 1) is expressed as a percentage of the total alkaloids (TIC—total ion current). The area of the GC–MS peak depends not only on the concentration of the corresponding compound but also on the intensity of its mass spectral fragmentation. Although data given in Table 1 do not express a real quantification, they can nevertheless be used for a relative comparison of the alkaloids.

Quantification of galanthamine in H. papilio The quantification was performed in triplicate using 50 mg of dried material (leaves and bulbs, separately) and codeine as i.s. (50 lg) in screw-top 2.0 ml Eppendorf tubes. The maceration procedure was carried out with 1 ml of MeOH adjusted to pH 8 with NH3 (25 %, v/v). After 2 h of extraction at room temperature assisted by 15 min ultrasonic baths every 30 min, the samples were centrifuged at 10,000 rpm for 2 min. An aliquot of 500 ll of methanolic macerate was acidified with 500 ll of H2SO4 (2 %, v/v) and neutral material removed with chloroform (2 9 500 ll). The aqueous fraction was then basified with 200 ll of NH3 (25 %, v/v) and alkaloids extracted with CHCl3 (3 9 500 ll). Finally, the purified alkaloid extract was dried under N2 and redissolved in 100 ll of CHCl3 for GC–MS analysis. The GC–MS conditions were the same used for the alkaloid-rich extract (Section GC–MS and identification of alkaloids).

Recovering and repeatibility of the extraction The extraction recovery was performed as described above by adding 50, 300 and 500 lg of galanthamine to the dry plant sample (50 mg of powdered bulbs and leaves of H. papilio) before the extraction and purification. Intraday (n = 4) and interday (n = 8) repeatability was calculated with 50 mg of dried powdered bulbs of H. papilio, extracted, purified and analysed via GC–MS on two different days according to Berkov et al. (2008b).

Samples for X-ray

Narwedine (31) and 11b-hydroxygalanthamine (32) were dissolved in CHCl3 under a pentane atmosphere and left in the freezer (less than 5 C) for a week. Sanguinine (28) was dissolved in a

MeOH:EtOH mixture (1:1, v/v) under a pentane atmosphere and left in the freezer (less than 5 C) for two weeks. Galanthamine (27) was dissolved in Me2CO and left in the freezer for a week. Suitable crystals for X-ray analysis were preselected under a light microscope. The crystallographic data of 27 and 31 were in agreement with those previously reported (Carrol et al. 1990; Hemetsberger et al. 2004).

X-Ray analysis for sanguinine (28)

A translucent prism-like specimen of sanguinine with the dimensions 0.192 mm 9 0.278 mm 9 0.457 mm was used for X-ray crystallographic analysis. First, the X-ray intensity data were determined, with a total of 171 frames collected at an exposure time of 1.71 h. The frames were integrated with the Bruker SAINT software package using a narrow-frame algorithm. The integration of the data using a monoclinic unit cell yielded a total of 19,735 reflections to a maximum h angle of 30.67 (0.70 A ° resolution), of which 7366 were independent (average redundancy 2.679, completeness = 94.1 %,Rint = 4.80 %, Rsig = 5.54 %) and 6597 (89.56 %) were greater than 2r(F2). The final cell constants of a = 9.227(6) A ° , b = 15.095(8) A ° , c = 9.750(5) A ° , b = 102.28(3) , volume = 1327.(2) A ° 3, are based upon the refinement of the XYZcentroids of 142 reflections above 20 r(I) with 4.944 \2h\49.15 . Data were corrected for absorption effects using the multi-scan method (SADABS). The ratio of minimum to maximum apparent transmission was 0.757.

The structure was solved and refined using the Bruker SHELXTL Software Package, with Z = 2 for the formula unit, C16H19NO3. The final anisotropic full-matrix least-squares refinement on F2 with 375 variables converged at R1 = 4.08 %, for the observed data and wR2 = 10.17 % for all data. The goodnessof- fit was 1.047. The largest peak in the final difference electron density synthesis was 0.382 e-/A ° 3 and the largest hole was -0.274 e-/A°3 with an RMS deviation of 0.058 e-/A° 3. On the basis of the final model, the calculated density was 1.367 g/cm3 and F(000), 584 e-.

X-Ray analysis for 11b-hydroxygalanthamine (32)

A prismatic crystal (0.1 9 0.09 9 0.08 mm) was selected and mounted on a MAR345 diffractometer with an image plate detector. Unit-cell parameters were determined from 107 reflections (3\h\318) and refined by the least-squares method. Intensities were collected with graphite monochromatized Mo Ka radiation. 8529 reflections were measured in the range 2.44 B h B 24.10, 2419 of which were non-equivalent by symmetry (Rint(on I) = 0.045). 2135 reflections were assumed as observed applying the condition I[2r (I). Lorentz-polarization was considered, but no absorption corrections were made. The structure was solved by direct methods, using the SHELXS computer program (Sheldrick 2008) and refined by the full-matrix least-squares method with the SHELX97 computer program (Sheldrick 2008), using 8529 reflections, (very negative intensities were not assumed). The function minimized was R w ||Fo|2 - |Fc|2 |2, where w = [r2(I) ? (0.0683P)2]-1, and P = (|Fo|2 ? 2 |Fc|2)/3, f, f' and f'' were taken from International Tables of X-Ray Crystallography (1974). All H atoms were computed and refined, using a riding model, with an isotropic temperature factor equal to 1.2 times the equivalent temperature

factor of the atom which are linked. The final R(on F) factor was 0.047, wR(on |F|2) = 0.117 and goodness of fit = 1.069 for all observed reflections. The number of refined parameters was 200. Max. shift/esd = 0.00, mean shift/esd = 0.00. Max. and min. peaks in final difference synthesis were 0.395 and -0.169 e.A° -3, respectively.

AChE inhibitory activity

The assay for measuring AChE inhibitory activity was performed as described by Lo´pez et al. (2002). Galanthamine hydrobromide was used as a positive control. A solution of the initial alkaloid-rich extract (chloroform fraction) at 1 mg/ml was taken up in MeOH and diluted further with phosphate buffer to give 100, 10, 1, 0.1, 0.01, 0.001 lg/ml solutions. Only IC50 values less than 100 lg/ml were considered. Compounds 27, 28, 31, and 32 were used in dilutions at the range of 10-8 to 10-3 M. Dilutions at 10-4 M were prepared in MeOH and further dilutions were carried out using phosphate buffer. IC50 of all extracts/compounds were measured in triplicate and the results are presented as a mean ± standard deviation using the software package Prism (Graph Pad Inc., San Diego, USA).

Results and discussion

GC–MS results

GC–MS analysis has here proved to be a robust and efficient technique for the rapid identification and quantification of a large number of alkaloids from Amaryllidaceae plant extracts. In this study, nine Brazilian species were analysed and thirty-six compounds belonging to seven skeleton-types were identified (see Fig. 1; Table 1).

Lycorine- and homolycorine-type: an 'ortho-para' phenolic coupling

As the lycorine skeletal-type is widely distributed in the Amaryllidaceae, it was surprising to find few representatives of this group in the Hippeastrum species and Rodophiala bifida surveyed. The alkaloid lycorine (3) is known to be poorly soluble in both CHCl3 and MeOH, which impedes its correct quantification by GC–MS (de Andrade et al. 2012). This might explain the low relative percentage observed for H. santacatarina (19.18 %, see Table 1), in contrast with a recent study of the same species, in which it was isolated as the main compound (Giordani et al. 2011b). Overall, homolycorine-type alkaloids were observed in higher variety and quantity, indicating that conversion of lycorine- to homolycorine-type alkaloids is an active chemical transformation in these species.

Crinine-, haemanthamine-, tazettine-, narciclasine- and montanine-type alkaloids: a 'para-para' phenolic coupling

A major mechanistic consideration in the biosynthesis of Amaryllidaceae alkaloids is 'para-para' coupling, since it gives rise to five distinct skeleton-types. The crinine-type skeleton is uncommon in the genus Hippeastrum and the absolute configuration of its 5,10b-ethano bridge is ratified only by CD spectra or X-ray crystallography (Wagner et al. 1996). As shown in Table 1 and Fig. 1, the 5,10b-ethanophenanthridinealkaloids described in this study possess the haemanthamine- type skeleton as previously confirmed (da Silva et al. 2008; de Andrade et al. 2011; Giordani et al. 2011a).

With respect to the tazettine skeleton, there are important features concerning epimerisation at C-3. Duffield et al. (1965) showed that the stereochemistry of the substituent at C-3 effects marked variations in the relative abundance of ions in EI-MS spectra. The b-configuration of the methoxyl group at C-3 facilitates a Retro-Diels–Alder (RDA) process in ring-B and loss of the neutral fragment [C5H8O], yielding diagnostic ion peaks at 247 and m/z 231 (M–84) for tazettine (19) and deoxytazettine (17), respectively. The fragment ion at m/z 70 is a small peak for both epimers (Duffield et al. 1965). As such, the ion peak at m/z 70 for criwelline and 16 is much more pronounced than those observed in 17 and 19, indicating that compound 16 is the 3-epideoxytazettine variant. The a-configuration of the 3-OMe substituent also induces a RDA fragmentation process, but in this case with the loss of the [C4H8N]? fragment, while the m/z 70 ion peak abundance establishes the C-3 configuration in tazettine derivatives (Duffield et al. 1965).

In general, montanine-type alkaloids are sparsely encountered and are thus poorly represented in the Amaryllidaceae. However, montanine (25) was here found as the main constituent in H. vittatum and R. bifida, while trisphaeridine (23) was the only representative of the narciclasine-type skeleton detectable as a minor compound or in trace amounts in most species (Table 1). Trisphaeridine has been considered a catabolic product (Bastida et al. 2006) and this hypothesis is supported by its presence in many species but hardly ever as the main alkaloid. Galanthamine-type alkaloids: a 'para-ortho' phenolic coupling Galanthamine-type compounds were found mainly in H. papilio and H. glaucescens, with galanthamine (27) being the main constituent in both cases (Table 1). Galanthamine was previously detected in H. papilio (de Andrade et al. 2011), but it is here reported for the first time in H. glaucescens. The remaining galanthamine-type representatives were detected in both species, but to a lesser extent. Miscellaneous alkaloids Ismine (34) and galanthindole (35) were identified in H. breviflorum, H. morelianum, H. psittacinum and H. glaucescens. Alkaloid 34, like 23, is also considered a catabolic product arising from the haemanthaminetype skeleton (Bastida et al. 2006). Galanthindole (35) and lycosinine B (36) have been considered representatives of a new skeleton containing a non-fused indole ring (U¨ nver 2007), although the possibility that they are artifacts of homolycorine- or tazettine-type derivatives cannot be overlooked.

Galanthamine quantification

H. papilio and H. glaucescens showed highest levels of galanthamine by GC–MS (Table 1) and the availability of H. papilio allowed the accurate quantification of galanthamine content from dried plant material. Bulbs and leaves exhibited values of 0.51 % (±0.012) and 0.33 % (±0.007), respectively (mg GAL/100 mg DW). These values are larger than those observed for Galanthus and Leucojum species used commercially by pharmaceutical companies for extraction of galanthamine (Cherkasov and Tolkachev 2002; Berkov et al. 2008b, 2009). The extraction recovery was 95 % (RSD 1.73 %), 93 % (RSD 2.20 %) and 91 % (RSD 0.81 %) for 50, 300 and 500 lg of added galanthamine, respectively. Intra-day repeatability (n = 4) expressed as RSD was determined as 1.60 for the first day and 2.21 for the second, while inter-day repeatability (n = 8) was 2.94 with adequate values of precision (RSD\5 %).

AChE inhibitory assay for alkaloid-rich extracts

The results from the microplate AChE inhibition assay of plant extracts are shown in Table 2. H. papilio and H. glaucescens presented the lowest IC50 values as determined via the Ellman method (Section ChE inhibitory activity). These are stronger activities than those observed for Galanthus elwesii and G. nivalis (at 0.1 and 10 lg/ml) as well as Leucojum aestivum (at 10 lg/ml) (Berkov et al. 2008c). The possibility of false-positive results in the AChE inhibitory activity values due to chemical inhibition (Rhee et al. 2003) should not be ruled out.

H. vittatum and R. bifida, in which elevated levels of montanine were detected, also exhibited notable AChE inhibitory effects (Table 2). Montanine (25) has previously demonstrated remarkable activity

against AChE obtained from rat brain, with more than 50 % inhibition at 1 mM (Pagliosa et al. 2010). These results, together with psychobiological activities reported earlier for montanine (da Silva et al. 2006), reinforce the potential of montanine-type derivatives as therapeutic candidates for AChE inhibition or other functions related to the central nervous system (da Silva et al. 2006; Pagliosa et al. 2010).

X-ray crystallography and AChE assay for galanthamine-derivatives

In agreement with previous reports (Lo´pez et al. 2002; Berkov et al. 2008c), galanthamine (27) and sanguinine (28) (Fig. 4) were the most active AChE inhibitory alkaloids (IC50s 0.35 and 0.06 lM, respectively). Narwedine (31) and 11b-hydroxygalanthamine (32) showed IC50 values of 9.38 and 3.49 lM, respectively. Some studies have been carried out to understand the binding of galanthamine and galanthamine-type alkaloids at the AChE active site (Bartolucci et al. 2001; Greenblatt et al. 1999). Although these have provided useful insights to the binding of the aromatic methoxyl group, the furan and cyclohexene rings as well as the 3-hydroxyl substituent, the effects of the N-methyl group remain largely unresolved. However, it is noteworthy that galanthamine adopted the same conformation at the active site gorge as that determined by X-ray crystallographic analysis (Bartolucci et al. 2001; Carrol et al. 1990).

The X-ray data obtained for galanthamine (27) and narwedine (31) are in agreement with previously published work (Carrol et al. 1990; Hemetsberger et al. 2004). The X-ray data for sanguinine (28)1 and 11b-hydroxygalanthamine (32)2 are reported here for the first time. Interestingly, narwedine (31) and 11bhydroxygalanthamine (32) (Fig. 2) showed an axial orientation for the NMe group, opposite to that seen for galanthamine. Sanguinine (28) (Fig. 3), the most potent AChE inhibitor known from the Amaryllidaceae, exhibited both orientations for the NMe group with 50 % of the molecules having the NMe group in the axial orientation and the other 50 % with the equatorial orientation. AChE inhibition curves together with the X-ray structures of all tested galanthamine alkaloids are shown in Fig. 4.

CONCLUSIONS

Some indigenous Brazilian species are shown to produce high quantities of the AChE inhibitors galanthamine and montanine. Following the approval of galanthamine by the FDA for clinical management of AD, galanthamine-type alkaloids have been the most commonly studied constituents of the Amaryllidaceae. Herein is reported for the first time the high levels of galanthamine detected via GC–MS in H. glaucescens. Galanthamine levels in leaves and bulbs of H. papilio were higher than those found in Leucojum, Galanthus and Narcissus, species traditionally used for commercial exploitation (Berkov et al. 2009). In addition, H. papilio and H. glaucescens extracts showed the lowest IC50 AChE inhibition values. Since evidence from docking studies of galanthamine analogs are inconclusive, further investigation is required to clarify the role of N-methyl orientation at the AChE active site gorge (Bartolucci et al. 2001). Galanthamine has the N-methyl group in an equatorial disposition and showed better AChE inhibitory activity than narwedine and 11b-hydroxygalanthamine, wherein the N-methyl group is axially-orientated. Chlidanthine also displays an axial orientation for the N-methyl group and exhibits noticeably lower AChE inhibition (IC50 24.1 lM) (Reyes-Chilpa et al. 2011). However, sanguinine exhibits the best IC50 inhibition values and has the N-methyl group in both axial and equatorial orientations. It is known that N-methyl conformers interchange rapidly in the naturally bound ligand, thereby restricting N-methyl orientation to a secondary role in new drug design. Nevertheless, further protein–ligand crystallography and protein–ligand docking studies should clarify the exact role of N-methyl orientation in galanthamine-type alkaloids.

References

Bartolucci C, Perola M, Christian P et al (2001) Three-dimensional structure of a complex of galanthamine (Nivalin) with acetylcholinesterase from Torpedo californica: implications for the drug design of new anti-Alzheimer drugs. Proteins 42:182–191

Bastida J, Lavilla R, Viladomat F (2006) Chemical and biological aspects of Narcissus alkaloids. In: Cordell GA (ed) The alkaloids, vol 63. Elsevier Inc, Amsterdam, pp 87–179

Berkov S, Codina C, Viladomat F et al (2008a) N-Alkylated galanthamine derivatives: potent acetylcholinesterase inhibitors from Leucojum aestivum. Bioorg Med Chem Lett 18:2263–2266

Berkov S, Bastida J, Nikolova M et al (2008b) Analysis of galanthamine-type alkaloids by capillary gas chromatography- mass spectrometry in plants. Phytochem Anal 19:285–293

Berkov S, Bastida J, Nikolova M et al (2008c) Rapid TLC/GCMS identification of acetylcholinesterase inhibitors in alkaloids extracts. Phytochem Anal 19:411–419

Berkov S, Georgieva L, Kondakova V et al (2009) Plant source of galanthamine: phytochemical and biotechnological aspects. Biotechnol Biotechnol Equip 23:1170–1176

Berkov S, Bastida J, Viladomat F et al (2011) Development and validation of a GC-MS method for a rapid determination of galanthamine in Leucojum aestivum and Narcissus ssp.: A metabolomic approach. Talanta 83:1455–1465

Carrol P, F urst GT, Han SY et al (1990) Spectroscopic studies of galanthamine and galanthamine methiodide. Bull Soc Chim Fr 127:769–780

Castilhos TS, Giordani RB, Henriques AT et al (2007) Avaliac ¸a˜o in vitro das atividades antiinflamato´ria, antioxidante e antimicrobiana do alcalo´ide montanina. Rev Bras Farmacogn 17:209–214

Cherkasov OA, Tolkachev ON (2002) Narcissus and other Amaryllidaceae as sources of galanthamine. In: Hanks G (ed) Medicinal and aromatic plants–industrial profiles: Narcissus and Daffodil, the genus Narcissus. Taylor and Francis, London and New York, pp 242–255

C¸ itog˘lu G, T anker M, Gu¨mu¨s¸el B (1998) Antiinflamatory effects of lycorine and haemanthidine. Phytother Res 12:205–206

da Silva AFS (2005) Hippeastrum vittatum (L'He´r) Herbert e Hippeastrum striatum (Lam.) Moore: Ana´lise quı´mica e avaliac¸a˜o biolo´gica dos alcaloides isolados. Dissertation, Universidade Federal do Rio Grande do Sul

da Silva AFS, de Andrade JP, Bevilaqua LR et al (2006) Anxiolytic-, antidepressant- and anticonvulsivant-like effects of the alkaloid montanine isolated from Hippeastrum vittatum. Pharmacol. Biochem Behav 85:148–154

da Silva AFS, d e Andrade JP, Machado KRB et al (2008) Screening for cytotoxic activity of extracts and isolated alkaloids from bulbs of Hippeastrum vittatum. Phytomedicine 15:882–885

de Andrade JP, Berkov S, Viladomat F et al (2011) Alkaloids from Hippeastrum papilio. Molecules 16:7097–7104

de Andrade JP, Pigni NB, Torras-Claveria L et al (2012) Bioactive alkaloids from Narcissus broussonetii: mass spectral studies. J Pharm Biomed Anal 70:13–25

Duffield AM, Aplin RT, Budzikiewicz H et al (1965) Mass spectrometry in structural and stereochemical problems. LXXXII. A study of the fragmentation of some Amaryllidaceae alkaloids. J Am Chem Soc 87:4902–4912

Giordani RB, Vieira PB, Weizenmann M et al (2010) Candimine-induced cell death of the amitochondriate parasite Trychomonas vaginalis. J Nat Prod 73:2019–2023

Giordani RB, de Andrade JP, Verli H et al (2011a) Alkaloids from Hippeastrum morelianum Lem. (Amaryllidaceae). Magn Reson Chem 49:668–672

Giordani RB, Vieira PB, WeizenmannMet al (2011b) Lycorine induces cell death in the amitochondriate parasite, Trichomonas vaginalis, via an alternative non-apoptotic death pathway. Phytochemistry 72:645–650

Greenblatt HM, Kryger G, Lewis T et al (1999) Structure of acetylcholinesterase complexed with (-)–galanthamine at 2.3 A ° resolution. FEBS Lett 463:321–326

Hemetsberger M, Treu M, Jordis U et al (2004) 1-methylgalanthamine derivatives. Monatsh Chem 135:1275–1287

International Tables of X-Ray Crystallography (1974) Kynoch Press. Birmingham

Kreh M, Matusch R, Witte L (1995) Capillary gas chromatography-mass spectrometry of Amaryllidaceae alkaloids. Phytochemistry 38:773–776

Lo´pez S, Bastida J, Viladomat F et al (2002) Acetylcholinesterase inhibitory activity of some Amaryllidaceae alkaloids and Narcissus extracts. Life Sci 71:2521–2529 Machocho AK, Bastida J, Codina C et al (2004) Augustamine type alkaloids from Crinum kirkii. Phytochemistry 65:3143–3149

Maelicke A, Samochocki M, Jostock R et al (2001) Allosteric sensitization of nicotinic receptors by galantamine, a new treatment strategy for Alzheimer's disease. Biol Psychiatry 49:279–288

McNulty J, Nair JJ, Codina C et al (2007) Selective apoptosisinducing activity of crinum-type Amaryllidaceae alkaloids. Phytochemistry 68:1068–1074

McNulty J, Nair JJ, Singh M et al (2009) Selective cytochrome P450 3A4 inhibitory activity of Amaryllidaceae alkaloids. Bioorg Med Chem Lett 19:3233–3237

Pagliosa LB, Monteiro SC, Silva KB et al (2010) Effect of isoquinoline alkaloids from two Hippeastrum species on in vitro acetylcholinesterase activity. Phytomedicine 17:698–701

Reyes-Chilpa R, Berkov S, Herna´ndez-Ortega S et al (2011) Acetyl-cholinesterase inhibiting alkaloids from Zephyranthes concolor. Molecules 16:9520–9533

Rhee IK, van Rijn RM, Verpoorte R (2003) Qualitative determination of false-positive effects in the acetylcholinesterase assays using thin layer chromatography. Phytochem Anal 14:127–131

Sebben C (2005) Investigac¸ao quı´mica e biolo´gica em Hippeastrum breviflorum Herb. (Amaryllidaceae). Dissertation, Universidade Federal do Rio Grande do Sul

Sheldrick GM (2008) A program for automatic solution of crystal structure refinement. Acta Crystallogr A 64:112–221

U¨nver N (2007) New skeletons and new concepts in Amaryllidaceae alkaloids. Phytochem Rev 6:125–135

Vrijsen R, Berghe DAV, Vlietinck AJ et al (1986) Lycorine: an eukaryotic terminator inhibitor? J Biol Chem 261:505–507

Wagner J, Pham HL, Do¨pke W (1996) Alkaloids from Hippeastrum equestre Herb. -5. Circular dichroism studies. Tetrahedron 52:6591–6600

Wagner C, Sefkow M, Kopka J (2003) Construction and application of a mass spectral and retention time index database generated from plant GC/EI-TOF-MS metabolite profiles. Phytochemistry 62:887–900

Zupko´ I, Re´thy B, Hohmann J et al (2009) Antitumor activity of alkaloids derived from Amaryllidaceae species. In Vivo 23:41–48

Legends to figures

Fig. 1 Alkaloids found in the Brazilian species

Fig. 2 ORTEP projection of 11b-hydroxygalanthamine (32)

Fig. 3 Top, a view of the molecular structure of compound 3. Bottom, the labeled core of the cubane. Bonds depicted in orange correspond to the short Cu–O distances inside the {Cu4O4} cage and the dashed red bonds show the H-bonds involving the coordinated water molecule

Scheme 3 ORTEP projection of sanguinine (28)

Fig. 4 Acetylcholinesterase inhibition curve and X-ray structures of sanguinine, galanthamine, 11b-hydroxygalanthamine and narwedine showing the N-methyl orientation

FIGURE 1

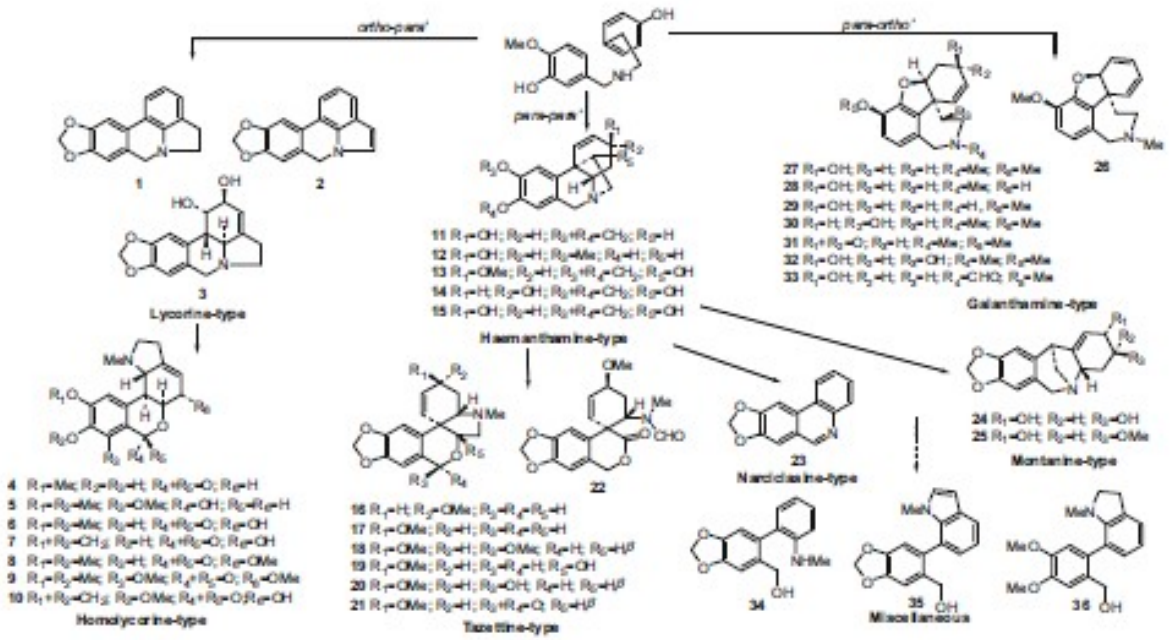
ortho-para'
para-para'
para-ortho'
Lycorine-type
Haemanthamine-type
Galanthamine-type
Homolycorine-type
Tazettine-type
Narciclasine-type
Montanine-type
Miscellaneous

FIGURE 2

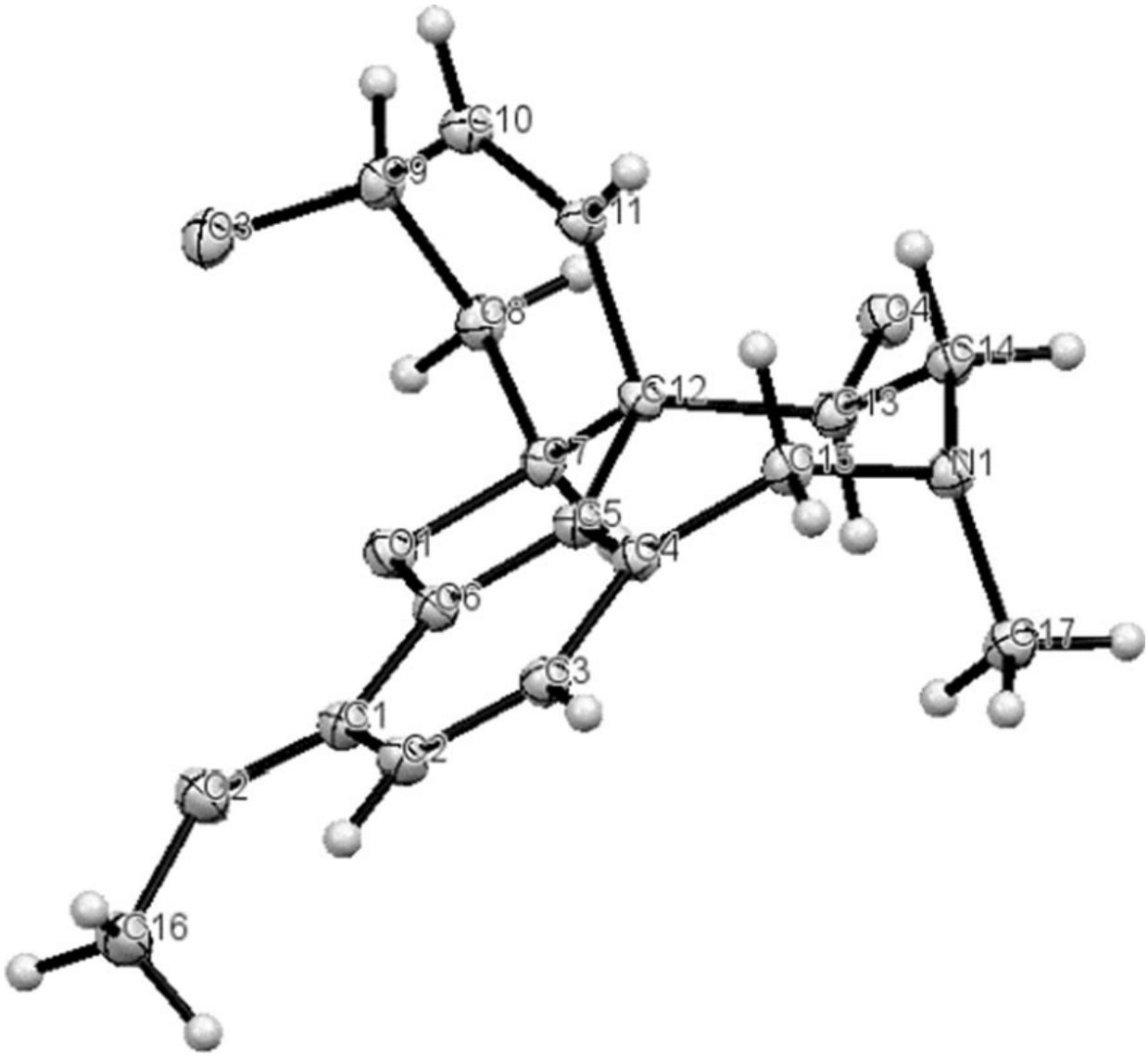
C10
C9
C11
O3
C8
O4
C14
C12
C13
C7
C15
N1
O1
C5
C4
C6
C17
C3
C1
C2
O2
C16

458 **FIGURE** 3

459

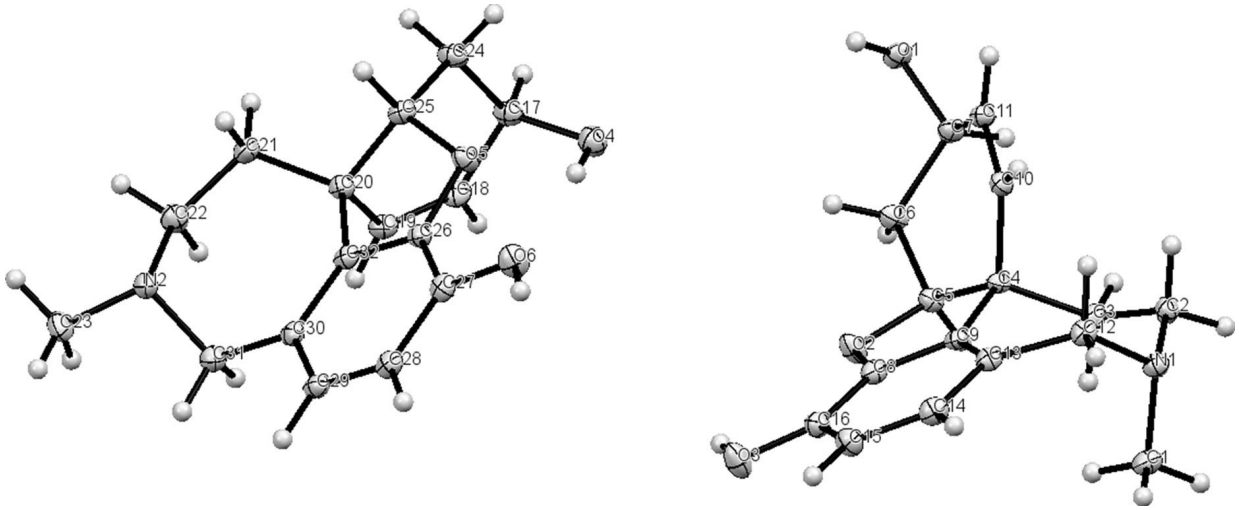

460

461

462 **FIGURE 4**

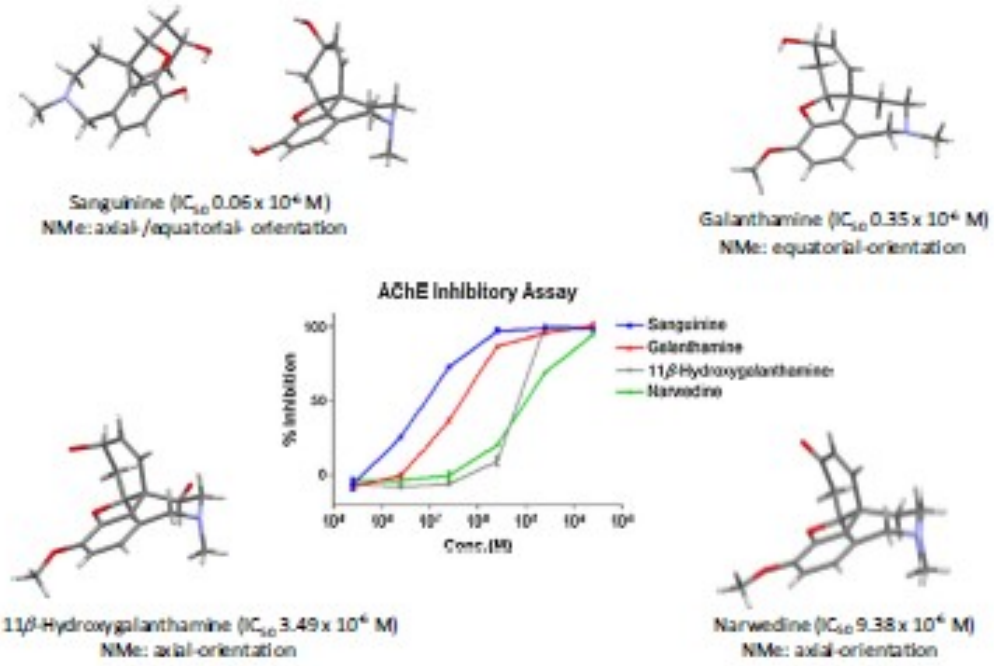

463

464

Table 1 Alkaloids found in several Brazilian species. Values are expressed as a relative percentage of TIC

Compound	RI	M^+	Rel. int. (%)	*H. striatum* Bulbs	*H. vittatum* Bulbs	*H. breviflorum* Bulbs	*H. morelianum* Bulbs	*H. papilio* Bulbs	*H. papilio* Leaves
Anhydrolycorine (**1**)	2501	251 (43)	250 (100), 192 (13), 191 (11), 165 (4), 164 (3), 139 (2), 124 (7)	–	tr	–	–	–	–
11,12-Dehydroanhydrolycorine (**2**)	2606	249 (60)	248 (100), 191 (10), 190 (24), 189 (7), 163 (7), 95 (17)	–	–	1.17	–	–	–
Lycorine (**3**)	2746	287 (31)	286 (19), 268 (24), 250 (15), 227 (79), 226 (100), 211 (7), 147 (15)	tr	0.60	–	–	–	–
8-*O*-Demethylhomolycorine (**4**)	2841	301 (–)	192 (0.5), 164 (2), 110 (8), 109 (100), 108 (23), 94 (3), 82 (3)	–	–	–	–	–	–
Nerinine (**5**)	2476	347 (–)	330 (7), 329 (3), 236 (1), 221 (9), 191 (2), 109 (100), 94 (2)	–	–	–	1.86	–	–
2α-Hydroxyhomolycorine (**6**)	2970	331 (–)	178 (3), 126 (8), 125 (100), 124 (7), 96 (31), 94 (4)	–	–	–	tr	–	–
Hippeastrine (**7**)	2917	315 (–)	190 (1), 162 (4), 134 (2), 125 (100), 96 (40), 82 (3)	–	–	–	–	–	–
2α-Methoxyhomolycorine (**8**)	2870	345 (–)	178 (5), 140 (11), 139 (100), 124 (67), 94 (7), 77 (5)	–	–	–	tr	–	–
2α,7-Dimethoxyhomolycorine (**9**)	2962	375 (–)	221 (2), 140 (9), 139 (100), 125 (6), 124 (55), 94 (4)	–	–	–	tr	–	–
Candimine (**10**)	3070	345 (–)	192 (1), 177 (2), 163 (1), 147 (1), 125 (100), 96 (30), 82 (2)				tr		
Vittatine (**11**)	2472	271 (100)	272 (20), 252 (35), 199 (70), 187 (61), 173 (22), 115 (28)	–	1.23	–	–	–	tr
8-*O*-Demethylmaritidine (**12**)	2510	273 (100)	274 (17), 230 (24), 201 (83), 189 (52), 175 (20), 115 (18)	–	1.62	–	–	tr	–
Haemanthamine (**13**)	2641	301 (13)	272 (100), 240 (16), 211 (13), 199 (7), 181 (21), 153 (8)	–	–	–	–	16.16	21.60
Hamayne (**14**)	2699	287 (5)	259 (18), 258 (100), 214 (10), 186 (14), 181 (14), 115 (13)	–	–	–	tr	–	–
11-Hydroxyvittatine (**15**)	2728	287 (6)	259 (18), 258 (100), 242 (10), 211 (15), 181 (20), 128 (13)	–	–	–	–	tr	–
3-Epideoxytazettine (**16**)	2241	315 (21)	300 (41), 232 (14), 231 (100), 185 (12), 115 (15), 70 (65)	–	–	3.12	7.55	–	–
Deoxytazettine (**17**)	2486	315 (21)	300 (15), 260 (5), 231 (100), 227 (10), 211 (15), 197 (10), 115 (9)	–	–	4.10	3.12	–	–

Table 1 continued

Compound	RI	M^+	Rel. int. (%)	*H. striatum* Bulbs	*H. virusum* Bulbs	*H. breviflorum* Bulbs	*H. morelianum* Bulbs	*H. papilio* Bulbs	*H. papilio* Leaves
6-Methoxypretazettine (**18**)	2610	345 (26)	330 (21), 262 (21), 261 (100), 239 (40), 228 (30), 201 (28)	–	–	tr	–	–	–
Tazettine (**19**)/Pretazettine (**20**)*	2653	331 (31)	316 (15), 298 (23), 247 (100), 230 (12), 201 (15), 181 (11), 152 (7)	–	–	26.50	58.83	–	–
3-Epimacronine (**21**)	2811	329 (27)	314 (23), 245 (100), 225 (14), 201 (83), 139 (16), 70 (18)	–	–	0.63	3.18	–	–
Tazettamide (**22**)	2914	313 (30)	260 (100), 229 (20), 201 (49), 171 (12), 143 (9), 115 (26)	–	–	–	tr	–	–
Trisphaeridine (**23**)	2282	223 (100)	222 (38), 167 (8), 165 (9), 164 (14), 138 (20), 137 (9), 111 (13)	tr	–	0.75	1.5	–	–
Pancracine (**24**)	2718	287 (100)	270 (22), 243 (22), 223 (25), 199 (29), 185 (34), 115 (18)	–	tr	–	–	–	–
Montanine (**25**)	2611	301 (100)	270 (90), 257 (39), 252 (26), 223 (33), 185 (37), 115 (30)	–	86.62	–	–	–	–
Anhydrogalanthamine (**26**)	1766	269 (100)	268 (38), 211 (43), 195 (22), 193 (31), 165 (61), 115 (26)	–	–	–	–	1.32	–
Galanthamine (**27**)	2395	287 (83)	288 (14), 286 (100), 270 (13), 244 (26), 216 (37), 174 (34)	tr	–	–	tr	63.24	58.97
Sanguinine (**28**)	2422	273 (100)	272 (79), 256 (18), 216 (18), 202 (37), 160 (44), 115 (25)	–	–	–	–	–	tr
N-Demethylgalanthamine (**29**)	2442	273 (98)	272 (100), 230 (44), 202 (34), 201 (12), 174 (13)	–	–	–	–	–	–
3-Epigalanthamine (**30**)	2443	287 (77)	286 (100), 270 (15), 244 (16), 216 (70), 211 (14), 174 (26)	–	–	–	–	–	–
Narwedine (**31**)	2483	285 (95)	284 (100), 242 (30), 228 (25), 216 (40), 199 (35), 174 (40)	–	–	–	–	1.62	2.85
11β-Hydroxygalanthamine (**32**)	2597	303 (24)	231 (21), 230 (100), 213 (27), 181 (13), 174 (13), 115 (15)	–	–	–	–	3.80	9.65
N-Formylnorgalanthamine (**33**)	2816	301 (100)	230 (9), 225 (16), 211 (18), 165 (9), 128 (10), 115 (13)	–	–	–	–	–	–
Ismine (**34**)	2280	257 (35)	238 (100), 211 (6), 196 (8), 168 (6), 154 (3), 106 (4), 77 (3)	–	–	1.41	0.75	–	–
Galanthindole (**35**)	2487	281 (100)	280 (7), 264 (13), 263 (17), 262 (20), 252 (15), 191 (14)	–	–	1.70	1.49	–	–
Lycosinine B (**36**)	2520	297 (100)	298 (19), 269 (72), 268 (56), 254 (32), 237 (19), 222 (16)	–	–	5.12	–	–	–

Table 1 continued

Compound	RI	M^+	Rel. int. (%)	*H. psittacinum* Bulbs	*H. psittacinum* Leaves	*H. santacatarina* Leaves	*H. glaucescens* Bulbs	*H. glaucescens* Leaves	*R. bifida* Bulbs
Anhydrolycorine (**1**)	2501	251 (43)	250 (100), 192 (13), 191 (11), 165 (4), 164 (3), 139 (2), 124 (7)	–	–	tr	–	–	–
11,12-Dehydroanhydrolycorine (**2**)	2606	249 (60)	248 (100), 191 (10), 190 (24), 189 (7), 163 (7), 95 (17)	–	–	14.64	–	–	–
Lycorine (**3**)	2746	287 (31)	286 (19), 268 (24), 250 (15), 227 (79), 226 (100), 211 (7), 147 (15)	–	–	19.18	–	–	–
8-*O*-Demethylhomolycorine (**4**)	2841	301 (–)	192 (0.5), 164 (2), 110 (8), 109 (100), 108 (23), 94 (3), 82 (3)	–	0.61	–	–	–	–
Nerinine (**5**)	2476	347 (–)	330 (7), 329 (3), 236 (1), 221 (9), 191 (2), 109 (100), 94 (2)	–	–	–	–	–	–
2α-Hydroxyhomolycorine (**6**)	2970	331 (–)	178 (3), 126 (8), 125 (100), 124 (7), 96 (31), 94 (4)	–	–	–	–	–	–
Hippeastrine (**7**)	2917	315 (–)	190 (1), 162 (4), 134 (2), 125 (100), 96 (40), 82 (3)	8.82	23.90	–	–	tr	–
2α-Methoxyhomolycorine (**8**)	2870	345 (–)	178 (5), 140 (11), 139 (100), 124 (67), 94 (7), 77 (5)	–	–	–	–	–	–
2α,7-Dimethoxyhomolycorine (**9**)	2962	375(–)	221(2), 140(9), 139(100), 125(6), 124(55), 94(4)	–	–	–	–	–	–
Candimine (**10**)	3070	345 (–)	192 (1), 177 (2), 163 (1), 147 (1), 125 (100), 96 (30), 82 (2)		–	–	–	–	–
Vittatine (**11**)	2472	271 (100)	272 (20), 252 (35), 199 (70), 187 (61), 173 (22), 115 (28)	–	–	tr	–	–	tr
8-*O*-Demethylmaritidine (**12**)	2510	273 (100)	274 (17), 230 (24), 201 (83), 189 (52), 175 (20), 115 (18)	–	–	–	–	–	–
Haemanthamine (**13**)	2641	301 (13)	272 (100), 240 (16), 211 (13), 199 (7), 181 (21), 153 (8)	–	–	3.61	–	–	–
Hamayne (**14**)	2699	287 (5)	259 (18), 258 (100), 214 (10), 186 (14), 181 (14), 115 (13)	–	–	–	–	–	–
11-Hydroxyvittatine (**15**)	2728	287(6)	259(18), 258(100), 242(10), 211(15), 181(20), 128(13)	–	–	8.51	–	–	–
3-Epideoxytazettine (**16**)	2241	315 (21)	300 (41), 232 (14), 231 (100), 185 (12), 115 (15), 70 (65)	–	–	–	1.26	–	–
Deoxytazettine (**17**)	2486	315 (21)	300 (15), 260 (5), 231 (100), 227 (10), 211 (15), 197 (10), 115 (9)	tr	0.82	tr	0.30	tr	tr

480
481
482
483
484
485

Table 1 continued

Compound	RI	M^+	Rel. int. (%)	*H. pittacinum* Bulbs	*H. pittacinum* Leaves	*H. santacatarina* Leaves	*H. glaucescens* Bulbs	*H. glaucescens* Leaves	*R. bifida* Bulbs
6-Methoxypretazettine (**18**)	2610	345 (26)	330 (21), 262 (21), 261 (100), 239 (40), 228 (30), 201(28)	–	–	–	–	–	–
Tazettine (**19**)/Pretazettine (**20**)*	2653	331 (31)	316 (15), 298 (23), 247 (100), 230 (12), 201 (15), 181 (11), 152 (7)	36.84	14.83	tr	7.62	14.89	tr
3-Epimacronine (**21**)	2811	329 (27)	314 (23), 245 (100), 225 (14), 201 (83), 139 (16), 70 (18)	5.78	7.31	tr	0.91	3.64	tr
Tazettamide (**22**)	2914	313 (30)	260 (100), 229 (20), 201 (49), 171 (12), 143 (9), 115 (26)	1.84	1.27	–	–	–	–
Trisphaeridine (**23**)	2282	223 (100)	222 (38), 167 (8), 165 (9), 164 (14), 138 (20), 137 (9), 111 (13)	1.16	tr	19.34	0.63	tr	–
Pancracine (**24**)	2718	287 (100)	270 (22), 243 (22), 223 (25), 199 (29), 185 (34), 115 (18)	–	–	–	–	–	–
Montanine (**25**)	2611	301 (100)	270 (90), 257 (39), 252 (26), 223 (33), 185 (37), 115 (30)	–	–	–	–	–	91.94
Anhydrogalanthamine (**26**)	1766	269 (100)	268 (38), 211 (43), 195 (22), 193 (31), 165 (61), 115 (26)	–	–	–	16.38	tr	–
Galanthamine (**27**)	2395	287 (83)	288 (14), 286 (100), 270 (13), 244 (26), 216 (37), 174 (34)	tr	tr	tr	55.30	65.15	–
Sanguinine (**28**)	2422	273 (100)	272 (79), 256 (18), 216 (18), 202 (37), 160 (44), 115 (25)	–	–	–	1.38	tr	–
N-Demethylgalanthamine (**29**)	2442	273 (98)	272 (100), 230 (44), 202 (34), 201 (12), 174 (13)	–	–	–	tr	–	–
3-Epigalanthamine (**30**)	2443	287 (77)	286 (100), 270 (15), 244 (16), 216 (70), 211 (14), 174 (26)	–	–	–	2.23	–	–
Narwedine (**31**)	2483	285 (95)	284 (100), 242 (30), 228 (25), 216 (40), 199 (35), 174 (40)	–	–	–	5.51	2.42	–
11β-Hydroxygalanthamine (**32**)	2597	303 (24)	231 (21), 230 (100), 213 (27), 181 (13), 174 (13), 115 (15)	–	–	–	–	–	–
N-Formylnorgalanthamine (**33**)	2816	301 (100)	230 (9), 225 (16), 211 (18), 165 (9), 128 (10), 115 (13)	–	–	–	–	tr	–
Ismine (**34**)	2280	257 (35)	238 (100), 211 (6), 196 (8), 168 (6), 154 (3), 106 (4), 77 (3)	13.9	10.46	–	–	2.10	–
Galanthindole (**35**)	2487	281 (100)	280 (7), 264 (13), 263 (17), 262 (20), 252 (15), 191 (14)	7.40	12.73	–	–	5.41	–
Lycosinine B (**36**)	2520	297 (100)	298 (19), 269 (72), 268 (56), 254 (32), 237 (19), 222 (16)	–	–	–	–	–	–

* Pretazettine (**20**) is quantified as tazettine (**19**) (de Andrade et al. 2012); Values <0.20 were assumed as "traces" (**tr**)

Table 2 AChE inhibitory activity of the alkaloid extracts

Plant species	IC_{50} (μg/ml)	AChE inhibition %	
		10 μg/ml	0.1 μg/ml
Hippeastrum striatum bulbs	nd	–	–
Hippeastrum vittatum bulbs	4.67	31.0	2.0
Hippeastrum breviflorum bulbs	nd	–	–
Hippeastrum morelianum bulbs	nd	–	–
Hippeastrum papilio bulbs	0.45	93.0	23.0
Hippeastrum papilio leaves	0.41	96.0	24.0
Hippeastrum psitaccinum bulbs	nd	–	–
Hippeastrum psitaccinum leaves	nd	–	–
Hippeastrum santacatarina bulbs	nd	–	–
Hippeastrum glaucescens bulbs	0.33	93.0	26.0
Hippeastrum glaucescens leaves	0.49	94.0	20.0
Hippeastrum aulicum leaves	nd	–	–
Rhodophiala bifida bulbs	8.45	28.0	3.0